Transition to burst synchronization in coupled neuron networks

Yu Shen,[1] Zhonghuai Hou,[1,2] and Houwen Xin[1]

[1]*Department of Chemical Physics, University of Science and Technology of China, Hefei, Anhui, 230026, People's Republic of China*

[2]*Hefei National Lab for Physical Science at Microscale, University of Science and Technology of China, Hefei, Anhui 230026, People's Republic of China*

(Received 16 September 2007; revised manuscript received 30 January 2008; published 25 March 2008)

Transition to burst synchronization (BS), where all the neurons start and end bursting simultaneously, has been studied on a diffusively coupled network of Hindmash-Rose bursting neurons. When the coupling strength ε is increased from zero, spatiotemporal chaos can be first tamed into one type of BS states with fold-homoclinic bursting, which then undergoes spike-adding and transits into another type of BS states with fold-Hopf bursting. The latter transition takes place via dynamic cluster separation, during which all the neurons with degree $k>k_c$ change to show fold-Hopf bursting, with εk_c nearly a constant. A reasonable mechanism behind such phenomena is given by using local mean field approximation, and the role of network topology is also discussed. The case when the neurons are coupled via chemical synapses is also briefly discussed.

DOI: 10.1103/PhysRevE.77.031920 PACS number(s): 87.19.lj, 05.45.Xt

In the last few years, synchronization of coupled oscillators on complex networks [1,2] has gained extensive attention due to its widespread importance in a variety of physical, biological, and chemical systems [3,4]. One of the frontiers has been the study of synchronization in coupled bursting neuron networks [5–11]. On one hand, synchronous neuron spike-bursting activity is particularly relevant for signal transmission and coding in the brain. For instance, the central pattern generator can produce regular, rhythmic bursting, while its individual neurons would show irregular bursts [12]. On the other hand, bursting is a typical phenomenon involving multi-time-scale dynamics, i.e., it occurs when neuron activity alternates, on a slow time scale, between a quiescent state and fast repetitive spiking [13,14]. Due to the existence of multiple time scales, interacting bursting neurons may show different forms of synchrony, including phase synchronization of spikes, *burst synchronization* (BS) when all the neurons start and end bursting simultaneously, and complete synchronization (CS). Therefore the explanation of such synchronous behaviors and revealing their roles in neurobiological science is a challenging problem of both practical and theoretical importance.

Regarding this issue, some important progress has been made recently. According to Pecora and Carroll [15], the stability of CS is determined by a so-called "master stability function" describing how the largest Lyapunov exponent transverse to the synchronization manifold depends on the topology of the network. Using this approach, Dhamala *et al.* have studied the transition to CS in coupled Hindmarsh-Rose (HR) networks, and they demonstrated that synchronization on the slow time scale is a precursor to CS and time delay can enhance neuron synchrony [5]. Belykh *et al.* reported an interesting result that in pulse-coupled Hindmarsh-Rose (HR) bursting neuron networks, the stability of the CS state only depends on the number of signals each neuron receives [6]. For BS, however, there is no such general stability rule. In a recent review, Izhikevich studied the synchronization of elliptic bursters via normal form equations [7]. By using a two-dimensional map, Rulkov [8] and others [9] have presented a mechanism for synchronized chaotic bursts, with or without external driving. Ivanchenko *et al.* have found the phase synchronization of burst neurons is not a singular function of coupling strength and can be break via spatiotemporal intermittency [10]. In a recent work [11], we have found that spatiotemporal chaos observed on a regular network of HR neurons can be tamed into ordered BS patterns, which are nearly periodic in time and almost synchronous in space. Since there are a lot of bursting mechanisms depending on how the rest and spiking state lose stability [7,13,14], the mechanism behind BS may differ from system to system and deserves more investigation. Furthermore, little is known about how the transition to BS happens and what the role of network topology is.

In the present paper, we study the transition from spatiotemporal chaos to BS patterns in a system of diffusively coupled chaotic HR neurons. The network is of small-world type constructed by randomly adding links to a regular chain. When coupling strength ε is increased from zero, spatiotemporal chaos can be tamed into BS patterns one after another, all are roughly periodic in time and nearly synchronous in space. Two types of transition between the BS patterns are observed: one via *spike-adding* and the other via change of bursting type from *fold-homoclinic* (FHC) to *fold-Hopf* (FH). The second transition takes place via dynamic cluster separation, in that all the neurons with degree $k>k_c$ will show FH bursting, and εk_c is shown to be nearly a constant. By using local mean field approximation, we demonstrate that these interesting phenomena can be explained by shrinking of homoclinic orbits in the fast subsystem of the HR neuron. We have also discussed briefly the case of synaptic coupling.

The system of diffusively coupled HR neurons is described by the following dynamic equations [5,10]:

$$\dot{x}_i = y_i - ax_i^3 + bx_i^2 - z_i + I_{\text{ext}} + \varepsilon \sum_j A_{ij}(x_j - x_i), \quad (1a)$$

$$\dot{y}_i = c - dx_i^2 - y_i, \quad (1b)$$

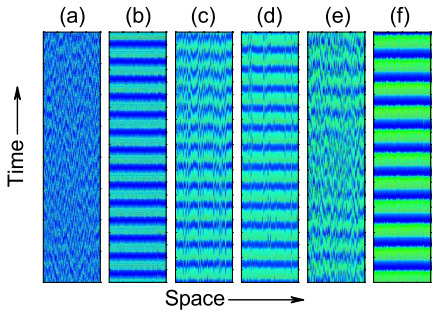

FIG. 1. (Color online) Transition from spatiotemporal chaos to BS patterns. From left to right, $\varepsilon=0.0002$, 0.0028, 0.0044, 0.0052, 0.0066, and 0.013, respectively.

$$\dot{z}_i = r[s(x_i - x_0) - z_i], \tag{1c}$$

where x represents the membrane action potential, and y and z are associated with fast and slow currents, respectively. The parameters are $a=1.0$, $b=3.0$, $c=1.0$, $d=5.0$, $r=0.006$, $s=4.0$, $x_0=-1.6$, and external current $I_{\text{ext}}=3.0125$, such that an isolated neuron is chaotic. $\mathbf{A}=(A_{ij})$ is the $n\times n$ connectivity matrix: $A_{ij}=1$ if neuron i is connected to neuron j, $A_{ij}=0$ otherwise, and $A_{ii}=0$. The network consists of N neurons with $N+M$ links between them, constructed by adding M random links to a regular ring. We fix the network topology and change the coupling strength ε.

Figure 1 shows the patterns observed on the network for $N=120$ and $M=1200$ for six different coupling strengths. Figure 1(a) is the spatiotemporal chaos observed for very weak coupling, Figs. 1(b), 1(d), and 1(f) are three types of BS patterns observed with the increment of ε, and Figs. 1(c) and 1(e) are transition patterns in between. In the BS patterns, the bursting of each neuron starts and ends nearly simultaneously, while the spikes inside them are asynchronous. For these patterns, the mean field is nearly periodic in time, i.e., the neuron population shows rhythmic behavior, even if an isolated one is chaotic. For further increased coupling strength ε, spikes get more and more synchronized until complete CS is achieved (not shown). Note that in the CS state, the neurons return to be chaotic and periodicity in time is lost [11].

To get more insight into the BS patterns, we have plotted the corresponding phase trajectories in the x-z plane, for one typically chosen single neuron, in Figs. 2(a)–2(c). Distinct features can be observed. On one hand, the spike amplitudes inside a burst in Figs. 2(a) and 2(b) are nearly constants, while in Fig. 2(c) it shrinks to zero before the trajectory returns to the quiescent state. On the other hand, the number of spikes per burst (SPB) in Fig. 2(a) is five and that in Fig. 2(b) is six. Therefore the transition from Fig. 1(b) to 1(d) takes place via spike-adding, while the transition from Fig. 1(d) to 1(f) involves a different bursting mechanism. Actually, one may understand the bursting behavior of a single HR neuron by the qualitative theory of a fast-slow system. The bifurcation geometry of the fast subsystem ($\dot{x}=y-ax^3+bx^2-z+I_{\text{ext}}, \dot{y}=c-dx^2-y$), by viewing the slow variable z as a control parameter, is drawn in Fig. 2(d). Quiescent and

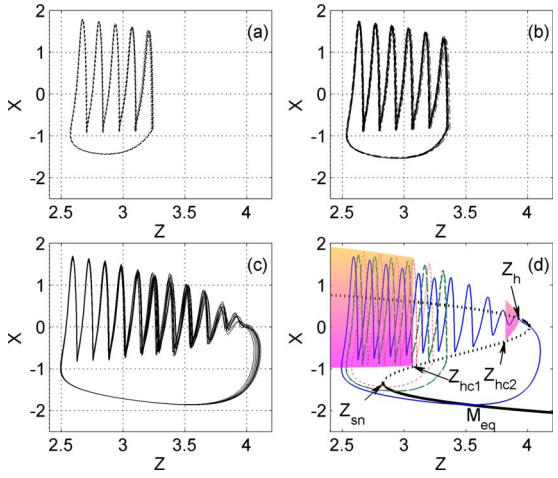

FIG. 2. (Color online) Typical phase trajectories of a single neuron for (a) $\varepsilon=0.0028$; (b) $\varepsilon=0.0052$; and (c) $\varepsilon=0.013$. (d) The bifurcation geometry of the fast subsystem viewing z as the control parameter, where the phase trajectories in (a)–(c) are redrawn in dotted, dashed, and solid lines, respectively.

spike states correspond to stable nodes in the lower branch of M_{eq} (the Z-shaped line consisting of equilibrium points of the fast subsystem), and stable limit cycles around the upper unstable branch of M_{eq}, respectively. When z changes slowly via Eq. (1c), jumps between quiescence and repetitive spiking would happen, leading to sustained bursts. The SPB number inside a burst depends on how long the system stays in the active state. For the parameters chosen here, the burst in an isolated HR neuron is of FHC type [7], i.e., the transition from quiescent state to repetitive spiking happens via fold bifurcation at Z_{sn}, while the spiking terminates via homoclinic bifurcation around Z_{hc1}. However, a distinctive feature shown in Fig. 2(d) is the existence of a second homoclinic bifurcation at Z_{hc2}, where stable limit cycles generated from Z_h terminate. If the HR neuron is perturbed in a way (as shown below) such that Z_{hc1} and Z_{hc2} move toward each other, two situations could happen: (i) Z_{hc1} and Z_{hc2} remain separated and the bursting type is still FHC; however, one or more spikes may emerge in a burst. This corresponds to the transition from Fig. 2(a) to 2(b), corresponding to the transition from Fig. 1(b) to 1(d). (ii) Z_{hc1} and Z_{hc2} collide such that the spiking states will lose stability via Hopf bifurcation at Z_h, the system will then show FH bursting [7]. This provides the transition mechanism from Fig. 2(b) to 2(c), and Fig. 1(d) to 1(f). The phase trajectories in Fig. 2(a) to 2(c) are redrawn in Fig. 2(d) for comparison.

Due to the existence of a clear characteristic burst time scale as shown in Figs. 1 and 2, one can define a "bursting phase" for each neuron as $\varphi_i(t)=2\pi(t-T_{i,k})/(T_{i,k+1}-T_{i,k})$, where $T_{i,k}$ is the moment at which the kth burst of neuron i starts. An order parameter can then be defined as $R=\left|\Sigma_{j=1}^{N}e^{i\varphi_j}\right|/N$ (Ref. [9]), and a larger R means more burst coherence among the neurons (for full BS state, $R=1$). In Fig. 3, the behavior of R (open circles) is plotted as a function of ε, indicating three phase transitions consistent with Fig. 1. The six points $A-F$ labeled in Fig. 3 correspond to Figs. 1(a)–1(f), respectively. The closed circles with error

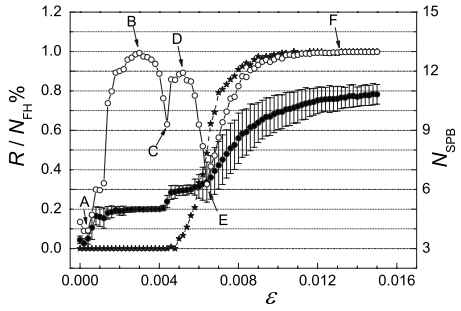

FIG. 3. Order parameter R (open circle), average number of spikes per burst N_{SPB} (closed circle), and fraction of neurons with FH-bursting N_{FH}/N (star) presented as functions of the coupling strength ε.

bars represent the SPB number (N_{SPB}) for a given ε, calculated as the number of circles around the upper branch of M_{eq} and averaged over time and neurons. Spike-adding can be clearly seen during the transition from point B to D. During the transition from point D to F, some neurons show FHC bursting and others show FH bursting. The fraction of neurons with FH bursting, N_{FH}/N, increases from 0 to 100% inside this range, as also shown in Fig. 3 (stars).

As demonstrated in Fig. 2(d), the observed transitions via spike-adding or changing of bursting type may be caused by the move and collision of homoclinic orbits at Z_{hc1} and Z_{hc2}. In the following part, we show that coupling can indeed provide such a mechanism, given the network is large and random enough. Actually, we can rewrite Eq. (1a) in the form

$$\dot{x}_i = y_i - ax_i^3 + bx_i^2 - \varepsilon k_i x_i - z_i + I_{\mathrm{ext}} + \varepsilon k_i \bar{x}_i, \qquad (1a')$$

where k_i is the degree of neuron i, and $\bar{x}=\Sigma A_{ij}x_j/k_i$ defines a local mean field (LMF). Hence k_i and $\bar{x}_i$ fully determine the behavior of neuron i. A key observation in our simulation is that the spiking states are almost *incoherent* among the neurons in the BS states. In the case that each neuron has enough neighbors, this incoherence makes $\bar{x}_i$ fluctuate slightly around a mean value $\bar{x}_{i0}$ (close to zero in the present study) in the spiking state. Our simulation also shows that $\bar{x}_i$ depends weakly on i in the BS states. According to Eq. (1a′), x_i will then be "dragged" toward this LMF, which will reduce the spike amplitude and the two homoclinic orbits will shrink and move closer. The parameter $\alpha_i \equiv \varepsilon k_i$ determines the strength of such a dragging. It is then helpful to study the bursting behavior of a perturbed HR system: $\dot{x}=y-ax^3+bx^2-\alpha x-z+I_{\mathrm{ext}}+\alpha\bar{x}_0$, $\dot{y}=c-dx^2-y$, $\dot{z}=r[s(x-x_0)-z]$, where $\bar{x}_0$ is a small constant. The main features are that N_{SPB} is not well-defined for $\alpha<\alpha_1$ (the system is chaotic) and that a periodic window exists in the region $\alpha\in(\alpha_1,\alpha_2)$ where N_{SPB} is 5; then N_{SPB} changes from 5 to 6 in a small chaotic window $\alpha\in(\alpha_2,\alpha_3)$, after which N_{SPB} remains 6 until the bursting type changes from FHC to FH at α_4. For $\bar{x}_0=0$, these values are $\alpha_1\approx 0.047$, $\alpha_2\approx 0.099$, $\alpha_3\approx 0.11$, and $\alpha_4=0.14$. Therefore when coupling strength increases (α increases), the behavior of a given neuron coupled to its LMF may undergo spike-adding and then a change of bursting type. This provides a reasonable mechanism for the shrinking and collision of homoclinic orbits and thus the transition between different BS patterns.

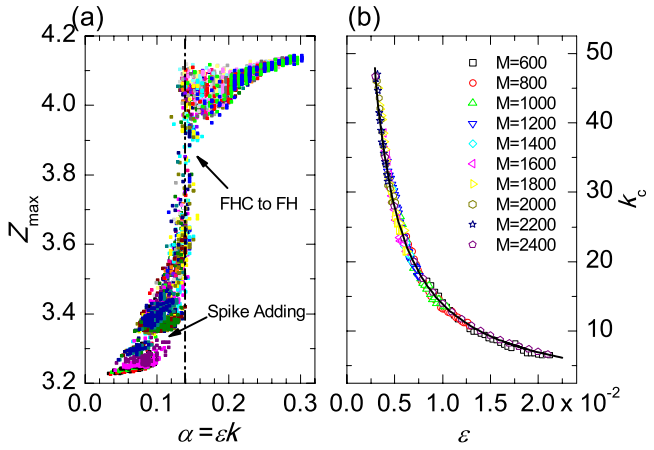

FIG. 4. (Color online) (a) $z_{\max}$ of all the neurons presented as a function of $\alpha=\varepsilon k$ during the spike-adding and burst-type transition, $M=1200$. (b) Dependence of k_c on ε for networks with different number of links; the line is $\varepsilon k_c=0.14$. $N=120$.

To test the LMF approximation, we have studied in detail the transition from Fig. 1(d) to 1(f). In this region, $\bar{x}_i$ is found to be approximately 0. If the LMF approximation applies, the bursting feature of a given neuron i will only depend on the parameter $\alpha_i=\varepsilon k_i$. Hence for a given ε, those neurons with $k_i \geq k_c=\alpha_4/\varepsilon$ will form one "dynamic cluster" with FH bursting, and the others will show FHC bursting. We found that this is exactly the case for the network considered here, as demonstrated in Fig. 4(a), where the maximum value of z for a neuron, $z_{\max}$, is drawn as a function of εk. A sharp transition occurs at $\varepsilon k\approx 0.14$, to the right side of which $z_{\max}$ is large, indicating FH type of bursting (see Fig. 2). Note that we have collected the data for different coupling strengths in the transition range D to F (see Fig. 2), and they collapse. The observed value 0.14 shows excellent agreement with α_4 obtained from the LMF approximation. In addition, we have performed similar analysis on networks with $N=120$ and M ranging from 600 to 2400, and all the obtained k_c values as a function of ε collapse very well to a curve $\varepsilon k_c=0.14$, as demonstrated in Fig. 4(b). The above analysis can be further extended to the region of spike-adding transition. For a given coupling strength, those neurons with a large degree will have one more SPB than those with a small degree. This is also demonstrated in Fig. 4(a), where a clear gap exists in the vicinity of $\alpha=0.1$. The transition region is different from $(0.099, 0.11)$ obtained from the LMF analysis with $\bar{x}_0=0$, mainly because that $\bar{x}_i$ was found to be oscillatory and deviated from zero in this range.

Based on the above analysis, one can figure out how these findings would depend on the network topology. A few points can be addressed. (i) In order that LMF approximation is valid, each neuron should have many *random* neighbors. (ii) In this case, BS patterns with 5 SPB like Fig. 1(b) can be observed if $\alpha_1<\varepsilon k_i<\alpha_2$ ($\forall\ i$) can be satisfied for some ε. Similarly, one requires $\alpha_3<\varepsilon k_i<\alpha_4$ ($\forall\ i$) to be satisfied in order to observe a 6 SPB BS pattern like Fig. 1(d). Therefore the network should be homogeneous enough to observe a BS

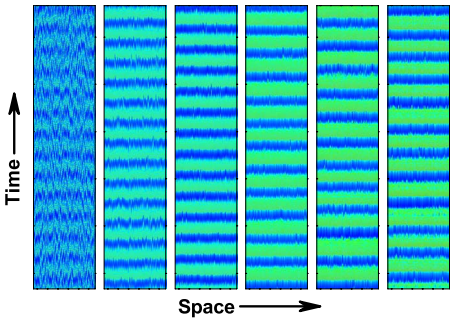

FIG. 5. (Color online) Transition from chaos to BS patterns for a chemical synapse with parameters $V_s=2$ and $\Theta_s=-0.25$. From left to right, $\varepsilon=0.0025$, 0.0100, 0.0175, 0.0250, 0.0325, and 0.0400, respectively.

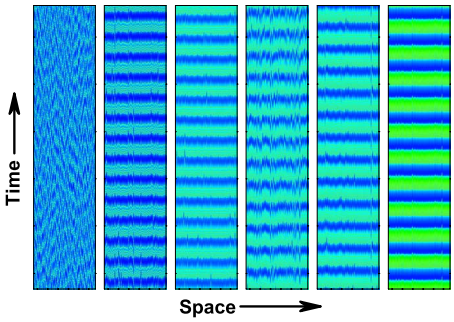

FIG. 6. (Color online) Transition from chaos to BS patterns for the chemical synapse with parameters $V_s=0$ and $\Theta_s=-1$. From left to right, $\varepsilon=0.000$, 0.001, 0.002, 0.003, 0.004, and 0.020, respectively.

pattern with FHC bursting. (iii) On the other hand, to observe a BS pattern with FH bursting like Fig. 1(f), $\varepsilon k_i > \alpha_4$ ($\forall\ i$) must be fulfilled; and in addition, ε should be smaller than the threshold ε_c for complete synchronization determined by the master stability function (for the network considered here, $\varepsilon_c \approx 0.56$ [16]). In a word, a large homogeneous HR network with many random links in between may undergo transition from spatiotemporal chaos to BS patterns with FHC bursting or FH bursting.

It is worthy here to compare our results to previous studies on the dynamics of coupled bursting neurons. In Ref. [8], Rulkov used a two-dimensional map model to study the mechanism of "chaotic regularization," which is essentially the BS state. Therein, the author also utilized a fast-slow decomposition of the whole system, and spike-incoherence in the firing state played an important role for the regularization, which is similar to our study here. In Ref. [9], the author proposed a "network mechanism" for BS, using the same model as in Ref. [8]. It was shown that as the coupling strength is increased, the synchronization is first lost via a kind of "spatial intermittency," and with further increased coupling strength a fast spiking appears resulting in BS. Such a spike-adding process is quite similar to our result, although the fact that neurons with more degree burst with more pieces first, as elucidated clearly in the present work, was not investigated there. In Ref. [6], Belykh *et al.* studied the onset of full-synchronization of coupled HR neurons and they found that the neuron degree did "matter," a result being quite consistent with ours, though here we considered the transition to BS.

In the present work, we have mainly considered the case of diffusive coupling which applies to electric synapses. For chemical synapses, the neurons are often pulse-coupled as in Ref. [6], i.e., the action potential of a given neuron will be dragged to a reverse potential (excitatory or inhibitory) by its neighbors that have action potentials above a given threshold. In such a case, the dynamics is more complicated than that for diffusive coupling, and the observed phenomenon depends on the choice of the model parameters such as the reversal potential and threshold. For instance, we have studied the behavior of a synaptically coupled system where the first equation (1a) is replaced by the following:

$$\dot{x}_i = y_i - ax_i^3 + bx_i^2 - z_i + I_{\text{ext}} + \varepsilon(V_s - x_i)\sum_j A_{ij}\Theta(x_j), \tag{1a''}$$

where V_s is the reversal potential, $\Theta(x_j)$ is the Heaviside function, which is 1 for $x_j > \Theta_s$ and 0 otherwise. Similar to the diffusive-coupling case, we have also observed typical transitions from spatiotemporal chaos to the BS state, as shown in Figs. 5 and 6 for $(V_s=2, \Theta_s=-0.25)$ and $(V_s=0, \Theta_s=-1)$, respectively. In addition, a spike-adding process is also observed, as indicated by the phase portraits depicted in Figs. 7 and 8. For synaptic coupling, the membrane potentials are now "dragged" to the reversal potential instead of shrinking to the local mean field $\bar{x}_i$. Although the value of the reversal potential is different from $\bar{x}_i$, the meeting point of stable cycles and the nullcline M_{eq} will move right so that more spikes will be generated in a burst. However, taking another look at Figs. 7 and 8, we find that the transition from FHC to FH bursting does not necessarily happen. For $(V_s=2, \Theta_s=-0.25)$, the synapse is excitatory and the

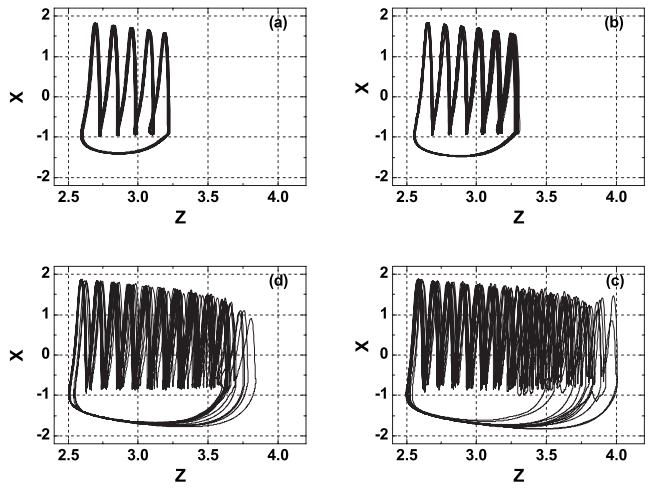

FIG. 7. Typical phase portraits of a single neuron for chemical synapses with parameters $V_s=2$ and $\Theta_s=-0.25$. From (a) to (d), $\varepsilon=0.0025$, 0.01, 0.0325, and 0.04, respectively. Spike-adding is observed, but no transition to FH bursting happens.

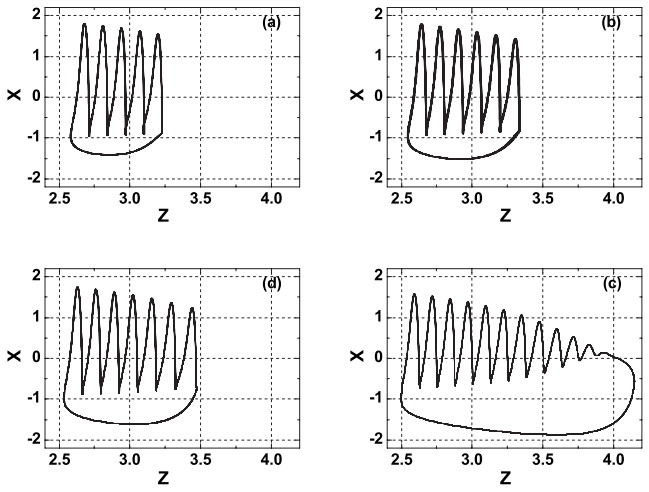

FIG. 8. Typical phase portraits of a single neuron for chemical synapses with parameters $V_s=0$ and $\Theta_s=-1$. From (a) to (d) $\varepsilon=0.001$, 0.002, 0.004, and 0.02, respectively. Spike-adding and transition to FH bursting are both observed.

reversal potential V_s is larger than $x_i(t)$ for any neuron at any time, such that the stable cycles are "dragged up" without shrinking. As shown in Fig. 7, transition to FH bursting does not occur in this case. However, if the reversal potential is close to 0, which lies in the neighborhood of the upper branch of M_{eq}, the spikes will be "dragged" to this nullcline, and the transition to FH bursting would also happen, as demonstrated in Fig. 8. Note that although the transition to FH bursting could happen in certain situations, the LMF approximation is not valid because the threshold mechanism destroys the "spike-incoherence." How to qualitatively explain the observations under such synaptic coupling theoretically would deserve more studies in future work.

In conclusion, we have studied the transition from spatiotemporal chaos to burst synchronization (BS) in a diffusively coupled network of bursting neurons. The BS patterns are nearly periodic in time, although each isolated neuron is chaotic. More than one type of BS patterns are observed, transitions between which take place via spike-adding or change of bursting type. During the transitions, the neurons are separated into different dynamic clusters, characterized by the number of spikes per burst or the burst mechanism. We have also qualitatively explained the mechanism behind the transition, revealing that neuron degree plays a key role, by using a local mean field approximation and investigating the bifurcation geometry of the fast subsystem. To show comparison, we have also considered the case when the neurons are coupled via chemical synapses. Transition to BS and spike-adding can also be observed; however, transition between different types of bursting does not necessarily happen. Local mean field analysis also fails in this case. Since synchronous bursting plays an important role in signal processing in the brain, and coherent behavior of coupled multitime-scale systems are of great research interest, our study may find its application both in neurobiological science and the study of complex systems.

The work was supported by the National Science Foundation of China (Grants No. 20433050 and 20673106).

[1] For some review of complex networks, please see: S. H. Strogatz, Nature (London) **410**, 268 (2001); R. Albert and A. L. Barabási, Rev. Mod. Phys. **74**, 47 (2002); M. E. J. Newman, SIAM Rev. **45**, 167 (2003); S. Boccaletti, V. Latora, Y. Moreno, M. Chavez, and D.-U. Hwang, Phys. Rep. **424**, 175 (2006).

[2] D. J. Watts and S. H. Strogatz, Nature (London) **393**, 440 (1998); A. L. Barabási and R. Albert, Science **286**, 509 (1999).

[3] A. Pikovsky, M. G. Rosenblum, and J. Kurths, *Synchronization: A Universal Concept in Nonlinear Sciences* (Cambridge University Press, Cambridge, England, 2001).

[4] Mauricio Barahona and L. M. Pecora, Phys. Rev. Lett. **89**, 054101 (2002); F. Qi, Z. Hou, and H. Xin, *ibid.* **91**, 064102 (2003); T. Nishikawa, A. E. Motter, Y. C. Lai, and F. C. Hoppensteadt, *ibid.* **91**, 014101 (2003); M. Chavez, D. U. Hwang, A. Amann, H. G. E. Hentschel, and S. Boccaletti, *ibid.* **94**, 218701 (2005); A. Arenas, A. Diaz-Guilera, and C. J. Perez-Vicente, *ibid.* **96**, 114102 (2006).

[5] M. Dhamala, V. K. Jirsa, and M. Ding, Phys. Rev. Lett. **92**, 028101 (2004); **92**, 074104 (2004).

[6] I. Belykh, E. de Lange, and M. Hasler, Phys. Rev. Lett. **94**, 188101 (2005).

[7] E. M. Izhikevich, SIAM Rev. **43**, 315 (2001).

[8] N. F. Rulkov, Phys. Rev. Lett. **86**, 183 (2001).

[9] M. V. Ivanchenko, G. V. Osipov, V. D. Shalfeev, and J. Kurths, Phys. Rev. Lett. **98**, 108101 (2007).

[10] M. V. Ivanchenko, G. V. Osipov, V. D. Shalfeev, and J. Kurths, Phys. Rev. Lett. **93**, 134101 (2004).

[11] M. Wang, Z. Hou, and H. Xin, ChemPhysChem **7**, 579 (2006).

[12] R. C. Elson, A. I. Selverston, R. Huerta, N. F. Rulkov, M. I. Rabinovich, and H. D. I. Abarbanel, Phys. Rev. Lett. **81**, 5692 (1998).

[13] E. M. Izhikevich, N. S. Desai, E. C. Walcott, and F. C. Hoppensteadt, Trends Neurosci. **26**, 161 (2003).

[14] A. Shilnikov and G. Cymbalyuk, Phys. Rev. Lett. **94**, 048101 (2005); P. Channell, G. Cymbalyuk, and A. Shilnikov, *ibid.* **98**, 134101 (2007).

[15] L. M. Pecora and T. L. Carroll, Phys. Rev. Lett. **80**, 2109 (1998).

[16] The threshold of CS is determined by $\varepsilon_c\lambda_2=\beta$, where λ_2 is the largest nonzero eigenvalue of the Laplacian matrix of the network, and β is decided by the master stability function. For the present work, $\lambda_2=10.08$, and $\beta=0.87$, thus $\varepsilon_c\approx 0.086$.